

THE EFFECT OF HETEROGENEITY OF IN-SITU COMBUSTION: THE
PROPAGATION OF COMBUSTION FRONTS IN LAYERED POROUS
MEDIA

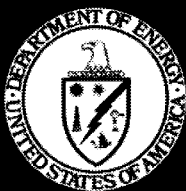
Topical Report
January 2002

By
I. Yücel Akkutlu
Yanis C. Yortsos

Date Published: June 2002

Work Performed Under Contract No. DE-AC26-99BC15211

University of Southern California
Los Angeles, California



**National Energy Technology Laboratory
National Petroleum Technology Office
U.S. DEPARTMENT OF ENERGY
Tulsa, Oklahoma**

DISCLAIMER

This report was prepared as an account of work sponsored by an agency of the United States Government. Neither the United States Government nor any agency thereof, nor any of their employees, makes any warranty, expressed or implied, or assumes any legal liability or responsibility for the accuracy, completeness, or usefulness of any information, apparatus, product, or process disclosed, or represents that its use would not infringe privately owned rights. Reference herein to any specific commercial product, process, or service by trade name, trademark, manufacturer, or otherwise does not necessarily constitute or imply its endorsement, recommendation, or favoring by the United States Government or any agency thereof. The views and opinions of authors expressed herein do not necessarily state or reflect those of the United States Government.

This report has been reproduced directly from the best available copy.

**The Effect of Heterogeneity of In-Situ Combustion:
The Propagation of Combustion Fronts in Layered Porous Media**

By
I. Yücel Akkutlu
Yanis C. Yortsos

June 2002

Work Performed Under DE-AC26-99BC15211

Prepared for
U.S. Department of Energy
Assistant Secretary for Fossil Energy

Jerry Casteel, Project Manager
National Petroleum Technology Office
P.O. Box 3628
Tulsa, OK 74101

Prepared by
Department of Chemical Engineering
University of Southern California
University Park Campus
HEDCO 316, USC
Los Angeles, CA 90089-1211

Table of Contents

Abstract	v
1. Introduction	1
2. Preliminaries: Combustion in a Single Layer	2
3. Combustion in a Two-Layered Porous Medium	7
4. Results	14
5. Concluding Remarks	22
References	23

Abstract

Large fractions of heavy oil reserves remain in shallow reservoirs, consisting of relatively thin sands separated by nearly impermeable shales. A potential recovery method for heavy oil is in-situ combustion. Compared to other methods, in situ combustion involves the added complexity of exothermic chemical reactions and temperature-dependent kinetics. Previous theoretical work by the authors have focused on the process in a single layer [7]. In this report we try to extend the approach to heterogeneous systems, by considering the simpler case of in-situ combustion in layered porous media (and particularly to a two-layer model). Analytical models are developed to delineate the combined effects of fluid flow, reaction and heat transfer on the dynamics of combustion fronts in layered porous media, using as parameters the thermal coupling between the layers, the heat transfer to the surroundings and the permeability contrast. We find that in layered systems, the thermal coupling between layers leads to coherent traveling fronts, propagating at the same velocity. This coupling retards greatly fronts in the more permeable layers and accelerates only slightly those in the less permeable ones, until a common front velocity is attained. As in the single-layer case, there exists a unique solution, under adiabatic conditions, and multiple steady-state solutions, under non-adiabatic conditions. The latter lead to ignition and extinction conditions. We show that the layer thickness and the permeability contrast between the layers play a crucial role. Importantly, for a sufficiently large permeability contrast, relatively small layer thickness and under non-adiabatic conditions, steady-state propagation in the two layers cannot be sustained, and the process becomes extinct, even though, under the same conditions, sustained propagation would have been predicted for the equivalent single-layer problem with the average injection velocity. Simple constraints are derived to delineate this case. The analysis is useful for the understanding of the viability of in situ combustion in heterogeneous porous media.

1 INTRODUCTION

The sustained propagation of a combustion front is necessary for the recovery of oil using in situ combustion. Compared to other methods, in situ combustion involves the complexity of exothermic reactions and temperature-dependent reaction kinetics. The combustion dynamics are influenced by the fluid flow of injected and produced gases, the heat transfer in the porous medium and the surroundings, the rate of combustion reaction(s) and the heterogeneity of the porous medium. In the presence of heat losses, the possibility exists of extinction (quenching) as well as the necessity of ignition for sustained propagation.

Combustion fronts in porous media have been studied extensively in the context of filtration combustion. Analytical treatments of the combustion front dynamics is possible, by using methods similar to the analysis of laminar flames (gaseous phase combustion in the absence of porous medium). Using the property that the activation energy of the overall reaction is large in comparison with the thermal enthalpy [1], Britten and Krantz [2, 3] provided an asymptotic analysis in one-dimensional systems of reverse combustion in coal gasification. In detailed works, Schult *et al.* [4, 5] investigated the adiabatic combustion of a homogeneous porous medium, in the contexts of fire safety and the synthesis of compacted metal powders (SHS processes). More recently, forward and reverse filtration combustion in a non-reacting porous medium was studied using a pore-network model by Chuan and Yortsos [6]. In parallel, a detailed analysis of the propagation of planar combustion fronts in porous media was undertaken by the present authors [7]. They addressed the issue of steady-state propagation under both adiabatic and non-adiabatic conditions, but emphasized the effect of heat losses to the surroundings. The latter were modeled both by conduction (for subsurface applications) and by convection (for laboratory applications). A number of important results were obtained, which are briefly summarized in the next section.

In this report, we consider the use of the same type of approach in an attempt to answer the important question of the effect of the porous medium heterogeneity on the sustained propagation of combustion fronts. As in other contexts, a simple representation of heterogeneity is through the use of layers. For example, layered systems have been employed to

investigate heterogeneity effects on processes such as miscible and immiscible displacement [8]. In the latter processes, the effect of heterogeneity typically enters through fluid mobility (where the displacement in a more permeable layer is further accelerated in the case of unfavorable mobility ratio, and conversely retarded in the case of a favorable mobility ratio). In the combustion case of interest here, however, the coupling enters through the heat transfer between the layers, to be expressed by a simple convective-type model. The assumption is rigorously valid if the layers are sealed from one another, or if the fluid mobility remains constant through the process, which is a good assumption, when the net rate of gas generation is small. Then, the injection rate in each layer is constant in time, and proportional to the layer permeability. The analysis will be conducted for two simple geometries, a two-layer system and a symmetric three-layer system, under both adiabatic and non-adiabatic conditions. Our emphasis is on understanding how the heat transfer coupling affects the front propagation in the different layers, on whether or not a state of coherent traveling fronts develops and on whether or not a sufficiently sharp permeability contrast can lead to the extinction of the process. Throughout the report, we will use methods similar to the single-layer problem of [7]. Because of the relevance of those results to the present problem, they are briefly summarized below.

2 PRELIMINARIES: COMBUSTION IN A SINGLE LAYER

Under adiabatic conditions, it is found that there is always sustained propagation, where the front temperature is given by

$$\theta_f \equiv T_f/T_o \approx 1 + q, \quad \text{where} \quad q = \frac{Q\rho_f^o}{(1-\phi)c_s\rho_s T_o} \quad (1)$$

we denoted the heat of reaction by Q , the initially available fuel content per total volume by ρ_f^o and the volumetric heat capacity of the porous medium by $(1-\phi)c_s\rho_s$. Clearly, equation (1) shows that the front temperature is practically independent of the front velocity.

Under non-adiabatic conditions, however, front temperature and front velocity are coupled. When the heat losses are modeled by heat conduction in semi-infinite surroundings, the temperature of the front is obtained from the different equation

$$\theta_f = 1 + \frac{q}{\omega^{2/3} z_1 - \omega^{4/3} \sqrt{z_1}} \quad \text{where} \quad \omega = \frac{2\alpha_s}{Hv_i} \quad (2)$$

and z_1 is the positive root of the algebraic equation

$$\frac{\bar{\mu}^2}{z_1} = (1 + \bar{\mu}z_1)^2, \quad \text{with} \quad \bar{\mu} = -\left(\frac{\omega}{V_D}\right)^{2/3}. \quad (3)$$

In (2), H is the thickness of the porous medium, v_i the injection velocity, $V_D = V/v_i$ is the dimensionless front velocity normalized with the injection velocity, and $\alpha_s = \lambda/(1 - \phi)c_s$ is the effective thermal diffusion coefficient. A similar equation applies for the convective heat losses case.

In all cases, the front velocity is related to the front temperature through the following equation

$$V_D^2 = \mathcal{A}\theta_f \exp\left(-\frac{\gamma}{\theta_f}\right) \left(\frac{1 - \mu V_D}{1 + \mu_g V_D}\right) \quad (4)$$

where $\gamma = E/RT_o$ is the Arrhenius number, E is the activation energy, R the universal gas constant, μ and $\mu_g = \mu_{gp} - \mu$ are dimensionless stoichiometric coefficients for oxygen and produced gas due to reaction, respectively (see [7] for more details), and

$$\mathcal{A} = \frac{a_s \alpha_s k_o Y_i p_i}{q E I_\eta v_i^2} \quad \text{where} \quad I_\eta = \int_0^1 \frac{(1 - \eta)}{\psi(\eta)} d\eta. \quad (5)$$

In addition, in Equation (5), a_s is the specific surface area per unit volume, k_o the pre-exponential factor, p_i the initial gas pressure, $\eta = 1 - \rho_f/\rho_f^o$ the extent of fuel conversion depth and $\psi(\eta)$ is a dimensionless function representing the dependence of reaction on η .

In the adiabatic case, there is always a solution for the front velocity as a function of the injection velocity. This relation is plotted in Figure 1 for typical parameter values. It shows

that the front velocity is proportional to the injection velocity at sufficiently small injection rates, and increases more slowly as the injection velocity becomes larger. In thermally decoupled layers, under adiabatic conditions, we should expect, therefore, that combustion fronts in high permeability layers would travel faster, according to the dynamics portrayed in Figure 1, for example.

On the other hand, in the non-adiabatic case, the coupling between velocity and temperature has significant implications. Figures 2 and 3 show results obtained for the front temperature versus the injection velocity for a varying thickness of the porous medium. The corresponding variation of the front velocity with the injection velocity is shown in Figure 4. For fixed thickness and injection velocity, the system typically shows multiplicity in the solutions, and for sufficiently thin layers, extinction and ignition points, E_c and I_c , exist in temperature (Figures 3, 2). As H decreases, the extinction threshold rapidly increases, namely it requires an increasingly larger injection velocity for the reaction to be sustained, as shown in the Figures. Between these thresholds, there exist three separate solutions for given injection and reservoir parameters, consisting of a stable low temperature (and velocity) branch in the vicinity of the initial conditions, a stable high temperature (and velocity) branch, where rigorous combustion takes place, and an unstable intermediate branch connected to the latter. Such behavior is typical of multiple solutions in other areas in reaction engineering. The upper branch is the solution corresponding to a proper combustion front. It approaches and runs parallel to the adiabatic solution. For a given H , the sensitivity of the front variables to the injection velocity is very large near the threshold, but becomes almost negligible above it. Likewise, the sensitivity of the extinction threshold E_c to the reservoir thickness is significant for values of H the order of 1 m or less, for the parameters assumed here. As H decreases, the extinction threshold rapidly increases, namely it requires an increasingly larger injection velocity for the reaction to be sustained, as shown in the Figures. Conversely, at larger H , the threshold decreases, and for sufficiently large values, multiplicity disappears altogether.

Analogous results are obtained when the heat losses are of the convective type, which would be appropriate for a laboratory application. In fact, in such cases, the system equations are simpler. One can combine the two applications [7], to obtain an expression for the effective

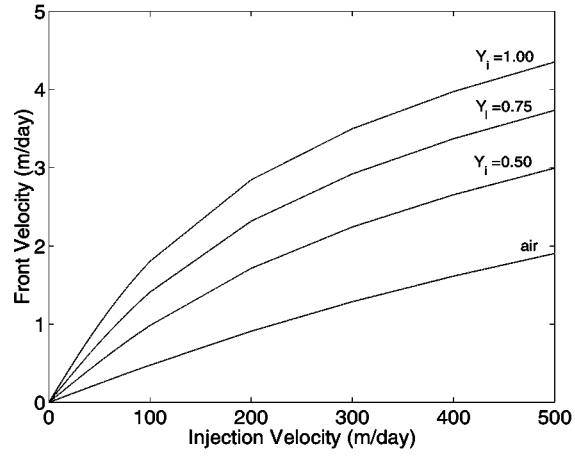


Figure 1: Steady-state front velocity versus injection velocity for different injected oxygen concentration for a single layer porous medium under adiabatic conditions.

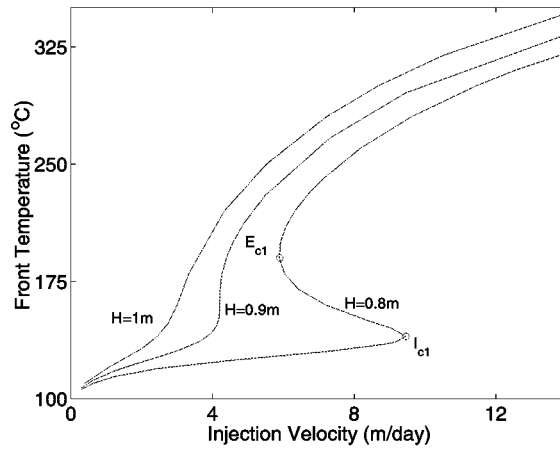


Figure 2: Front temperature versus injection velocity for a single layer under non-adiabatic conditions. $I_{c1}=(9.45,140.0)$, $E_{c1}=(5.9,190.0)$.

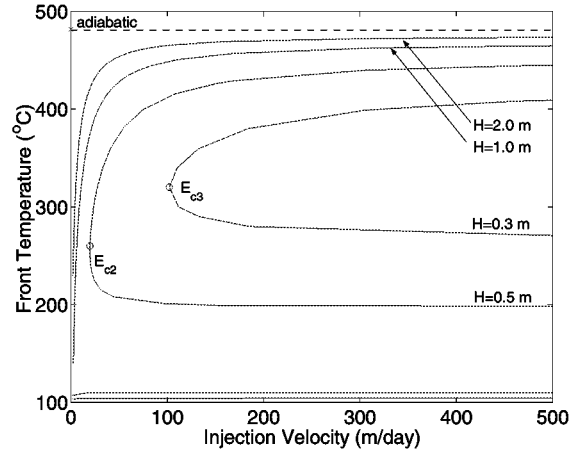


Figure 3: Front temperature versus injection velocity for a single layer under non-adiabatic conditions. $E_{c2}=(19.7,260.0)$, $E_{c3}=(102.1,320.0)$.

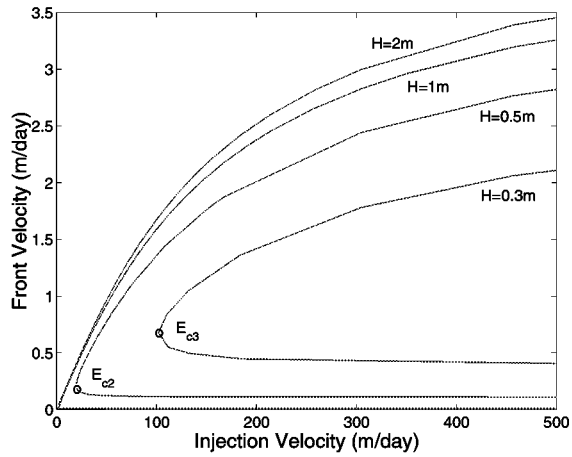


Figure 4: Front velocity versus injection velocity for a single layer under non-adiabatic conditions. $E_{c2}=(19.7,260.0)$, $E_{c3}=(102.1,320.0)$.

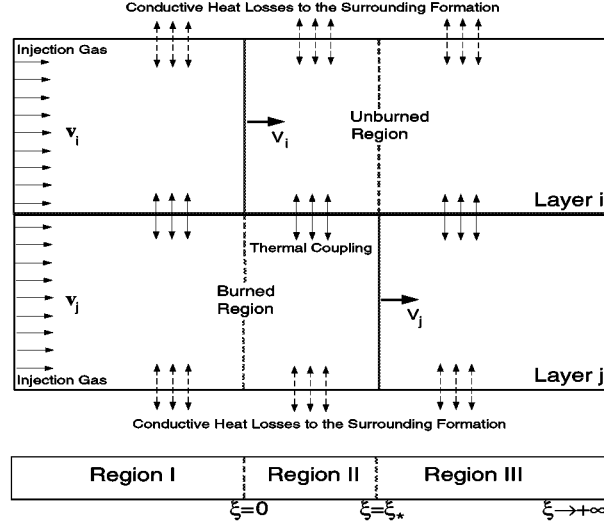


Figure 5: Schematic of the notation used for the propagation of combustion fronts in a two-layered porous medium.

heat transfer coefficient \tilde{h} in a system controlled by heat conduction. In terms of the Nusselt number, we have

$$\text{Nu} \equiv \frac{\tilde{h}H}{\lambda} = \frac{HV}{2\alpha_s} \left(\omega_i^{1/3} z_i^2 + 2\omega_i z_i^{3/2} + \omega_i^{5/3} z_i - \omega_i^{-1} \right) \quad (6)$$

Further details can be found in [7].

3 COMBUSTION IN A TWO-LAYERED POROUS MEDIUM

Consider, now, the application of the same approach to a layered porous medium. The first geometry to be considered is a two-layered system, as shown in the schematic of Figure 5.

The steady-state propagation of combustion in the two layers i and j is considered. The layers are homogeneous, but with different permeabilities (with layer j being more permeable), and hence different injection velocities. In the absence of mobility variation effects, these are proportional to the layer permeability. We assume only thermal coupling across the layers,

which will be expressed in terms of a convective-type heat model. Due to thermal coupling, it is apparent that isolated front propagation in each layer with front velocities dictated, e.g. by Figure 4, cannot take place. Indeed, we expect that the faster traveling front in layer j will slow down due to heat losses to layer i the front of which will accelerate until a coherent state is reached and the front velocities are the same in each layer. In the moving coordinate with respect to the combustion front, $\xi = x - V_D t$, where $x = \tilde{x}/l_*$ and $t = \tilde{t}/t_*$ are the dimensionless space and time variables with $l_* = \alpha_s/v_i$ and $t_* = l_*/v_i$, the dimensionless thermal energy balances for the two layers read

$$A_i \theta'_i = \theta''_i + \sigma(\theta_j - \theta_i) - h_i(\theta_i - 1) \quad (7)$$

$$A_j \theta'_j = \theta''_j + \sigma(\theta_i - \theta_j) - h_j(\theta_j - 1) \quad (8)$$

where prime denotes derivatives, and we have introduced

$$A_i = a \rho v_i - V_D \cong -V_D, \quad A_j = a \rho v_j - V_D \cong -V_D \quad (9)$$

The dimensionless parameter $a \ll 1$ represents the ratio of the volumetric heat capacity of the gas to the solid matrix, σ is the non-dimensional coefficient for the heat exchange between the two neighboring points in the direction transverse to the propagation, and we have also allowed for heat loss to the surroundings using the heat loss coefficients

$$h_i = \text{Nu} \left(\frac{\alpha_s}{H_i v_i} \right)^2, \quad h_j = \text{Nu} \left(\frac{\alpha_s}{H_j v_j} \right)^2 \quad (10)$$

The solution of this problem will be considered in the two different cases of adiabatic and non-adiabatic conditions.

3.1 Adiabatic conditions

In the adiabatic case, equation (8) simplifies to

$$\theta_i = \theta_j + \frac{1}{\sigma}(A_j\theta'_j - \theta''_j). \quad (11)$$

Inserted into equation (7) this gives the following differential equation

$$\theta_j^{(iv)} - B\theta_j''' + D\theta_j'' + \sigma B\theta_j' = 0, \quad (12)$$

where we defined

$$B = A_i + A_j, \quad D = A_i A_j - 2\sigma \quad (13)$$

Its solution is readily obtained,

$$\theta_j = \tilde{c}_0 + \tilde{c}_1 e^{r_1 \xi} + \tilde{c}_2 e^{r_2 \xi} + \tilde{c}_3 e^{r_3 \xi} \quad (14)$$

where $r_1 > 0$, $r_2, r_3 < 0$ are the real roots of

$$r^3 - Br^2 + Dr + \sigma B = 0 \quad (15)$$

The solution for θ_i follows using equation (11), namely

$$\begin{aligned} \theta_i = & \tilde{c}_0 + \tilde{c}_1 e^{r_1 \xi} + \tilde{c}_2 e^{r_2 \xi} + \tilde{c}_3 e^{r_3 \xi} \\ & + \frac{1}{\sigma} \left(A_j \left(\tilde{c}_1 r_1 e^{r_1 \xi} + \tilde{c}_2 r_2 e^{r_2 \xi} + \tilde{c}_3 r_3 e^{r_3 \xi} \right) - \tilde{c}_1 r_1^2 e^{r_1 \xi} - \tilde{c}_2 r_2^2 e^{r_2 \xi} - \tilde{c}_3 r_3^2 e^{r_3 \xi} \right). \end{aligned} \quad (16)$$

Because of the jump conditions at the two combustion fronts, it is convenient to consider three different regions, as shown in Figure 5. Using the far-field boundary conditions

$$\xi \rightarrow -\infty \quad : \quad \theta_i = \theta_j = \theta_I, \quad \xi \rightarrow \infty \quad : \quad \theta_i = \theta_j = 1 \quad (17)$$

we then have

I. Region I

$$\theta_i = \theta_I + c_1 e^{r_1 \xi} + \frac{1}{\sigma} \left(A_j c_1 r_1 e^{r_1 \xi} - c_1 r_1^2 e^{r_1 \xi} \right) \quad (18)$$

$$\theta_j = \theta_I + c_1 e^{r_1 \xi} \quad (19)$$

II. Region II

$$\begin{aligned} \theta_i = c_o + c_2 e^{r_1 \xi} + c_3 e^{r_2 \xi} + c_4 e^{r_3 \xi} \\ + \frac{1}{\sigma} \left(A_j \left(c_2 r_1 e^{r_1 \xi} + c_3 r_2 e^{r_2 \xi} + c_4 r_3 e^{r_3 \xi} \right) - c_2 r_1^2 e^{r_1 \xi} - c_3 r_2^2 e^{r_2 \xi} - c_4 r_3^2 e^{r_3 \xi} \right) \end{aligned} \quad (20)$$

$$\theta_j = c_o + c_2 e^{r_1 \xi} + c_3 e^{r_2 \xi} + c_4 e^{r_3 \xi} \quad (21)$$

III. Region III

$$\theta_i = 1 + c_5 e^{r_2 \xi} + c_6 e^{r_3 \xi} + \frac{1}{\sigma} \left(A_j \left(c_5 r_2 e^{r_2 \xi} + c_6 r_3 e^{r_3 \xi} \right) - c_5 r_2^2 e^{r_2 \xi} - c_6 r_3^2 e^{r_3 \xi} \right) \quad (22)$$

$$\theta_j = 1 + c_5 e^{r_2 \xi} + c_6 e^{r_3 \xi}. \quad (23)$$

To complete the problem requires formulating jump conditions across the combustion fronts.

These read as follows:

$$\xi = 0 \quad : \quad [\theta_i]_{\xi=0^-}^{\xi=0^+} = [\theta_j]_{\xi=0^-}^{\xi=0^+} = 0, \quad [\theta'_i]_{\xi=0^-}^{\xi=0^+} = -qV_{Di}, \quad [\theta'_j]_{\xi=0^-}^{\xi=0^+} = 0 \quad (24)$$

$$\xi = \xi_* \quad : \quad [\theta_i]_{\xi=\xi_*^-}^{\xi=\xi_*^+} = [\theta_j]_{\xi=\xi_*^-}^{\xi=\xi_*^+} = 0, \quad [\theta'_i]_{\xi=\xi_*^-}^{\xi=\xi_*^+} = 0, \quad [\theta'_j]_{\xi=\xi_*^-}^{\xi=\xi_*^+} = -qV_{Dj}. \quad (25)$$

Because the fronts travel with the same speed ($V_i = V_j$), both the front *and* the distance ξ_* between them must be determined. In essence, these constants are the eigenvalues of this system of ten equations (seven integration constants, ξ_* , V_D , and θ_I). In general, the system is non-linear, due to the intricate dependence between front velocity and heat transfer. The ten equations required for its solution consist of the 8 jump conditions, and the application of the expression (4) for the front velocity twice (note that this equation remains valid, regardless of the coupling between the two layers). Details for the solution are given in [9]. Numerical results will be discussed in a later section.

3.2 Non-adiabatic conditions

Working likewise, we can formulate the problem in the presence of heat losses. Now, additional terms describing the interaction with the surroundings must be included. Using equation (8) to substitute θ_i in terms of θ_j , we have

$$\theta_i = \left(1 + \frac{h_j}{\sigma}\right)\theta_j + \frac{1}{\sigma} \left(A_j\theta'_j - \theta''_j - h_j\right) \quad (26)$$

inserting into (7) and re-arranging we get

$$\theta_j^{(iv)} - B\theta_j''' + E\theta_j'' + F\theta_j' + G\theta_j - G = 0 \quad (27)$$

where

$$\begin{aligned} E &= A_i A_j - 2\sigma - (h_i + h_j) \\ F &= A_i(\sigma + h_j) + A_j(\sigma + h_i) \\ G &= h_i h_j + \sigma(h_i + h_j) \end{aligned} \quad (28)$$

the general solution of equation (27) is

$$\theta_j = 1 + \tilde{c}_1 e^{r_1 \xi} + \tilde{c}_2 e^{r_2 \xi} + \tilde{c}_3 e^{r_3 \xi} + \tilde{c}_4 e^{r_4 \xi} \quad (29)$$

where we have identified the real roots $r_1, r_2 > 0$ and $r_3, r_4 < 0$ of

$$r^4 - Br^3 + Er^2 + Fr + G = 0. \quad (30)$$

Again, we have to distinguish different expressions in different regimes, which are as follows:

I. Region I

$$\theta_i = 1 + \left(1 + \frac{h_j}{\sigma}\right) (c_1 e^{r_1 \xi} + c_2 e^{r_2 \xi}) + \frac{1}{\sigma} \left(A_j (c_1 r_1 e^{r_1 \xi} + c_2 r_2 e^{r_2 \xi}) - c_1 r_1^2 e^{r_1 \xi} - c_2 r_2^2 e^{r_2 \xi} - h_j\right) \quad (31)$$

$$\theta_j = 1 + c_1 e^{r_1 \xi} + c_2 e^{r_2 \xi} \quad (32)$$

II. Region II

$$\begin{aligned} \theta_i = 1 + \left(1 + \frac{h_j}{\sigma}\right) & (c_3 e^{r_1 \xi} + c_4 e^{r_2 \xi} + c_5 e^{r_3 \xi} + c_6 e^{r_4 \xi}) \\ & + \frac{1}{\sigma} \left(A_j \left(c_3 r_1 e^{r_1 \xi} + c_4 r_2 e^{r_2 \xi} + c_5 r_3 e^{r_3 \xi} + c_6 r_4 e^{r_4 \xi} \right) \right. \\ & \quad \left. - c_3 r_1^2 e^{r_1 \xi} - c_4 r_2^2 e^{r_2 \xi} - c_5 r_3^2 e^{r_3 \xi} - c_6 r_4^2 e^{r_4 \xi} - h_j \right) \end{aligned} \quad (33)$$

$$\theta_j = 1 + c_3 e^{r_1 \xi} + c_4 e^{r_2 \xi} + c_5 e^{r_3 \xi} + c_6 e^{r_4 \xi} \quad (34)$$

III. Region III

$$\theta_i = 1 + \left(1 + \frac{h_j}{\sigma}\right) (c_7 e^{r_3 \xi} + c_8 e^{r_4 \xi}) \frac{1}{\sigma} \left(A_j \left(c_7 r_3 e^{r_3 \xi} + c_8 r_4 e^{r_4 \xi} \right) - c_7 r_3^2 e^{r_3 \xi} + c_8 r_4^2 e^{r_4 \xi} - h_j \right) \quad (35)$$

$$\theta_j = 1 + c_7 e^{r_3 \xi} + c_8 e^{r_4 \xi}. \quad (36)$$

Application of the same jump conditions as before gives rise to a set of ten equations in terms of the ten unknowns (integration constants, the distance between the fronts and the front velocity). Details of the solution are found in [9].

3.3 Non-adiabatic, symmetric, three-layered porous medium

The same approach can be applied to the solution of a symmetric three-layered medium, when the two outer layers have the same properties. This type of geometry is useful in the investigation of the effect of a middle layer that plays the role of a permeable thief zone. Because of the symmetry assumed, velocity and temperature of the outer reaction fronts are taken to be identical, as shown in Figure 6.

Then, the governing energy balances become

$$A_i \theta'_i = \theta''_i + \sigma_i (\theta_j - \theta_i) - h_i (\theta_i - 1) \quad (37)$$

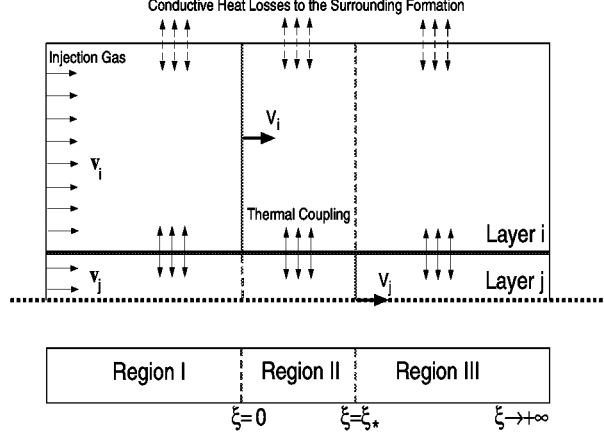


Figure 6: Schematic of the notation used for the propagation of combustion fronts in a two-layered porous medium.

$$A_j \theta_j' = \theta_j'' + \sigma_j (\theta_i - \theta_j). \quad (38)$$

Working as before, equation (38) gives θ_i ,

$$\theta_i = \theta_j + \frac{1}{\sigma_j} (A_j \theta_j' - \theta_j''). \quad (39)$$

Inserted into (37) gives

$$\theta_j^{(iv)} - B \theta_j''' + \bar{E} \theta_j'' + \bar{F} \theta_j' + \sigma h_i \theta_j - \sigma h_i = 0 \quad (40)$$

where

$$\bar{E} = A_i A_j - \sigma_i - \sigma_j - h_i$$

$$\bar{F} = B \sigma_j + A_j h_i$$

the solution of which is obtained as before, in terms of a combination of exponentials, with exponents the real roots $r_1, r_2 > 0$ and $r_3, r_4 < 0$ of the characteristic equation

$$r^4 - B r^3 + \bar{E} r^2 + \bar{F} r + \sigma_j h_i = 0. \quad (41)$$

The mathematical procedure is similar to the previous and will not be repeated (see [9] for more details).

4 RESULTS

The numerical solution was studied using typical in situ combustion data [7, 9]. Results were obtained for the temperature T_f and velocity V of the fronts as well as their distance $\tilde{\xi}_* = \xi_* \times l_*$, in terms of the velocity (hence, permeability) ratio $R = v_i/v_j$, the thermal coupling coefficient σ , the velocity of the layers, and, in the non-adiabatic cases, the layer thicknesses H_i and H_j . We considered two velocity cases, one in which the larger velocity is fixed to $v_j=100\text{m/day}$ (case j), and another in which lower velocity v_i is fixed to $v_i=100\text{m/day}$ (case i). In either case R was varied between its limits 0 and 1.

4.1 Adiabatic Two-layer Case

The procedure applied during the calculations is explained in detail in [9]. Figures 7 and 8 show the effect of R on the temperature profiles and the front velocity for constant σ , and case j. We note the following: The system recovers the single-layer solution (with $V=1.7346$ m/day) in the single-layer case $R = 1$ (Figure 7). Here the two fronts collapse, and their distance is nil. When $R = 0.5$ (Figure 8), the separation between the fronts is clear. The front in layer j has slowed down, and has a lower temperature than that of layer i , which has accelerated to a common velocity (equal to $V=1.0033$ m/day). The temperature profile is more diffuse than in the single-layer case, with heat being transferred from layer j to layer i downstream and from i to j upstream. Interestingly, the temperature profile in the lower-permeability layer has a peak, which is not present in the single-layer problem. Nonetheless, the far-field temperature upstream is equal to the adiabatic temperature. The common front velocity is much closer to the single-layer velocity for the lower-permeability layer (corresponding to an injection velocity of 50m/day, rather than the arithmetic average injection velocity of 75m/day). This reflects strong non-linear coupling effects. The effect of the thermal coupling parameter σ is shown in Figure 9. Interestingly, as σ decreases the coupling is not weakened, but rather enhanced. Clearly, the front separation has increases, the temperature peaks increased, while the common front velocity has further increased ($V=1.0161$ m/day).

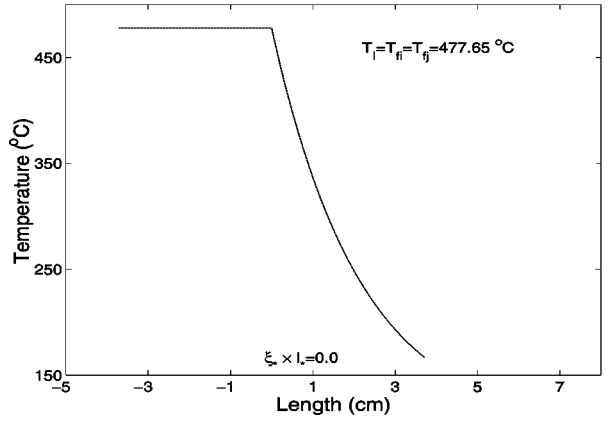


Figure 7: Temperature profiles for the two-layer adiabatic case. $R=1.0$, $\sigma=0.01$.

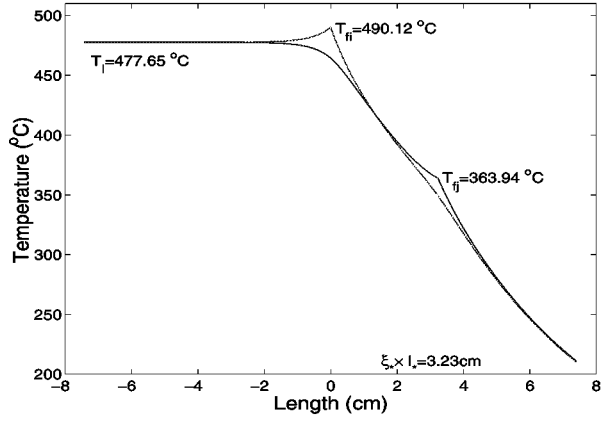


Figure 8: Temperature profiles for the two-layer adiabatic case. $R=0.5$, $\sigma=0.01$.

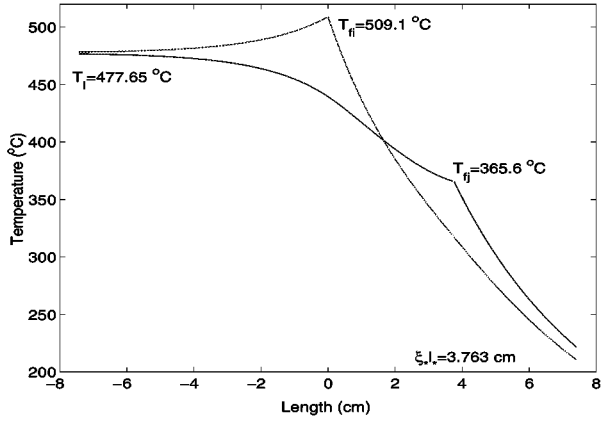


Figure 9: Temperature profiles for the two-layer adiabatic case. $R=0.5$, $\sigma=0.001$.

While these results point out to an important effect of R , the latter also depends on the actual velocity values. Figures 10-12 show two sets of the front temperatures, front velocities and front distance, as a function of R for $\sigma=0.01$ and the two cases j and i, respectively. Recall that case j corresponds to fixed $v_j=100$ m/day, while case i to fixed $v_i=100$ m/day. Of course, ideally one would like to have a three-dimensional plot with v_i and v_j as the independent variables. However, these computations can be time consuming and in the present we will restrict ourselves to only a few slices of this diagram.

It is clear from Figure 10 that the effect of the actual velocity levels is not great on the front temperatures (except for that of the leading front at small values of R). In fact, the far-field temperature behind the two fronts is not influenced at all by the variations in R or σ as its value is always the adiabatic temperature, as pointed out above. Thus, for the adiabatic case, the temperature is roughly only a function of R . However, the effect is significant on the front velocities and the front distance. In case j, where it is the larger injection velocity which is kept fixed, the front velocity decreases as the smaller injection velocity decreases, almost proportionally to it, while in case i, where the smallest velocity is fixed, the variation is insignificant. Analogous is the effect on the front distance.

These results suggest that essentially the behavior of the system is controlled by the layer with the smallest injection velocity, with the front velocity in particular almost being a slave of that variable. The implications of this finding are important. For the adiabatic case they simply affect the rate of front propagation. However, for the non-adiabatic case, discussed below, they may have more dramatic consequences, regarding the possibility of process extinction.

4.2 Non-adiabatic Two-layer Case

Using the formulation described in the previous sections, numerical results were obtained for the non-adiabatic case in the two-layer system. Now, in addition to the previous, an important additional parameter is the layer thickness, which was taken in all simulations shown as the same for the two layers.

When the layer thickness is sufficiently large (approximately 2m, for the parameters shown

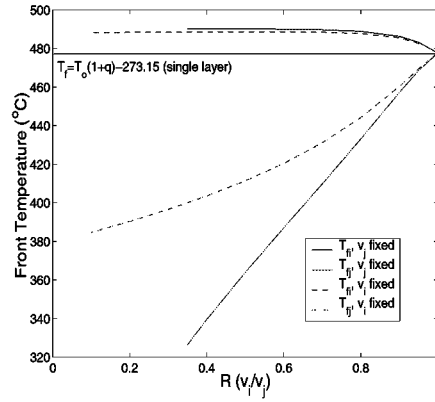


Figure 10: Front temperatures versus R for the two-layer adiabatic case. Solid lines denote case j, dashed lines denote case i.

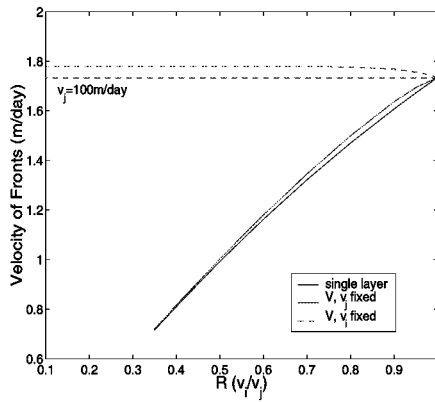


Figure 11: Front velocity versus R for the two-layer adiabatic case. Solid lines denote case j, dashed lines denote case i.

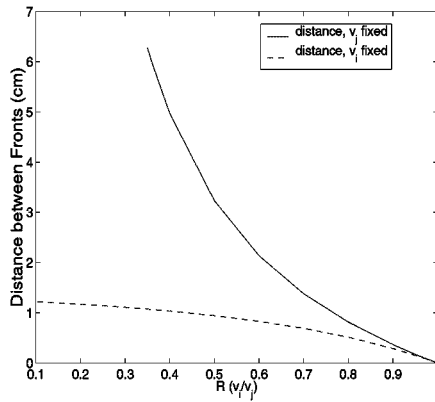


Figure 12: Distance between the fronts versus R for the two-layer adiabatic case. Solid lines denote case j, dashed lines denote case i.

here) the solution of the problem and its sensitivity to R and the velocities is qualitatively the same as in the adiabatic case. Unique solutions exist and the main difference is that the temperature profile is more spread out, has somewhat more structure and, of course, asymptotically tends to the initial value. Characteristic examples are shown in Figures 13-15. The observed similarity of the non-adiabatic model results when $H=2m$ to the results of the adiabatic case is consistent with the results of single layer analysis – the combustion fronts propagate as if the system is in the adiabatic mode, given that sufficient gas is injected into the layers.

On the other hand, when the thickness becomes small, the qualitative picture changes. As in the single-layer case, the possibility of multiplicity arises. Figures 16 and 17 show features very similar to the single layer. Thus, for case j, where the lower injection velocity can become sufficiently small in magnitude, extinction and ignition limits arise. The multiplicity arises simultaneously in both fronts, and both fronts ignite and get extinct simultaneously. The corresponding curves for case j are similar both qualitatively and quantitatively to the single layer case. The results for case i are somewhat different. Here, because the lowest velocity remains fixed (at 100 m/day), multiplicity does not arise until the layer thickness is sufficiently small (contrast Figures 16 and 17). By comparing with the single-layer results, this effect is somewhat unexpected. If we were to assume that the front basically follows the front velocity corresponding to the lower injection velocity, the curves corresponding to case i could be interpreted from the single-layer results as those corresponding to the upper branch. This would mean that intermediate and lower branches would also exist. These do not appear in Figure 16, although they do in Figure 17, which corresponds to a smaller thickness layer. One infers that when the velocities are sufficiently large, the composite, two-layer system behaves as one with an effectively larger thickness, compared to the case when the layer velocities are relatively small. This interpretation is also supported in the velocity and front distance curves shown in Figures 18 and 19. However, and contrary to the adiabatic case, another effect is also present here, namely, an intrinsic heterogeneity effect through the parameter R . For example, the above figures illustrate through case i, that by increasing the heterogeneity of the layers, extinction will eventually set in, even though the lower-permeability layer has

a fixed injection velocity. This effect is non-trivial and unexpected. For completeness, we examined the sensitivity of these results to the thermal parameter σ . Very small differences were found as σ was decreased by a factor of 10.

The implications of these results are important. They point out that increasing the permeability contrast between the layers can have dramatic effects on the propagation of a combustion front. Namely, given an overall injection rate, and for sufficiently small layer thickness, there is a sufficiently large permeability contrast, such that the process becomes extinct. Depending on the parameters, this contrast can be as low as 10. Strongly layered (and by extension, strongly heterogeneous) systems may thus be not good candidates for in-situ combustion. The above results gave only one indication of the ballpark values for this to occur. A more systematic analysis would require the development of 3-D plots using the two velocities as coordinates and the resulting identification of extinction and ignition limits.

4.3 Non-adiabatic Three-layer Case

For completeness, we also analyzed the symmetric, three-layer geometry. Now, the middle layer is shielded and does not lose heat directly to the surroundings. The results obtained were qualitatively similar to the previous non-adiabatic problem. In this geometry, we investigated the sensitivity of the results to the ratio of the thickness of the two layer, which here were taken unequal. In the calculations, we also kept the injection velocity of the surrounding layers fixed, and varied v_j (case i). Front temperature results are shown in Figure 20. It is shown that when the shielding layers are thick enough (dashed lines in Figure 20) the behavior approaches the adiabatic case, where there exists a unique solution. If the layer thickness decreases, then multiplicity sets in, with characteristics similar to the ones discussed above.

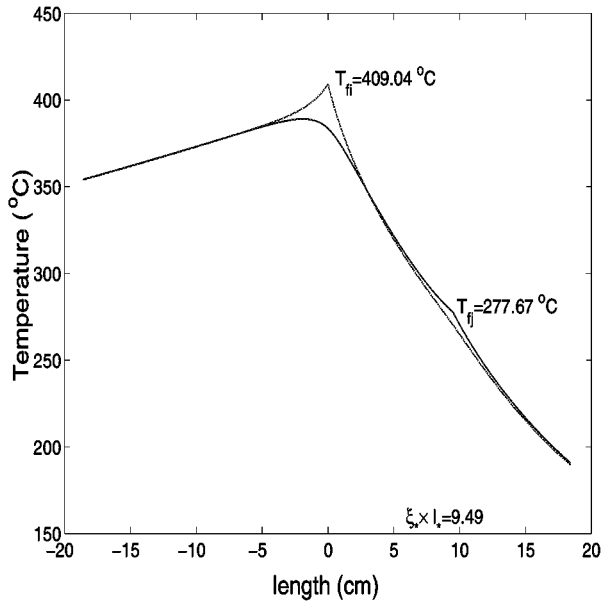


Figure 13: Temperature profiles for the non-adiabatic two-layer model. $H_i=H_j=2\text{m}$, $R=0.20$, $\sigma=0.01$, calculated $V=0.4070$ m/day.

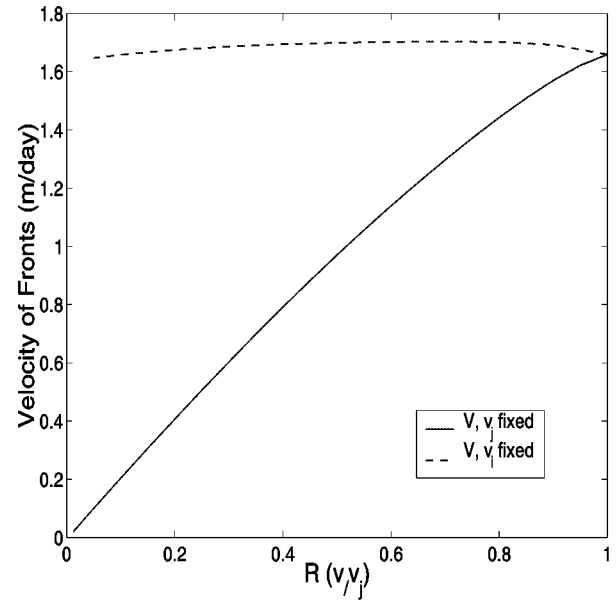


Figure 15: Velocity of the fronts versus R for the non-adiabatic two-layer model. Solid lines denote case j, dashed lines denote case i. $H_i=H_j=2\text{m}$, $\sigma=0.01$.

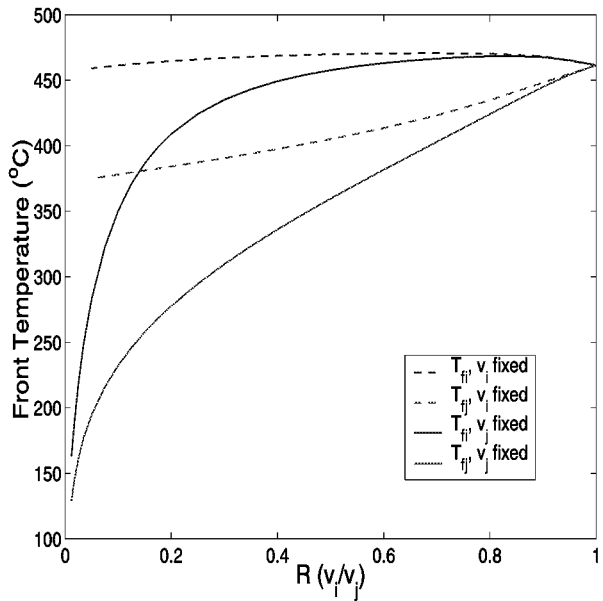


Figure 14: Front temperatures versus R for the non-adiabatic two-layer model. Solid lines denote case j, dashed lines denote case i. $H_i=H_j=2\text{m}$, $\sigma=0.01$.

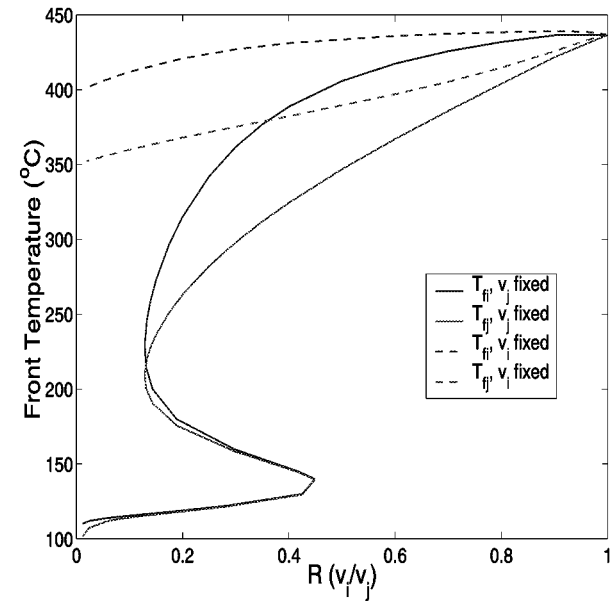


Figure 16: Nonadiabatic front temperatures for layers i and j versus R . Solid lines denote case j, dashed lines denote case i. $H_i=H_j=0.8\text{m}$, $\sigma=0.1$.

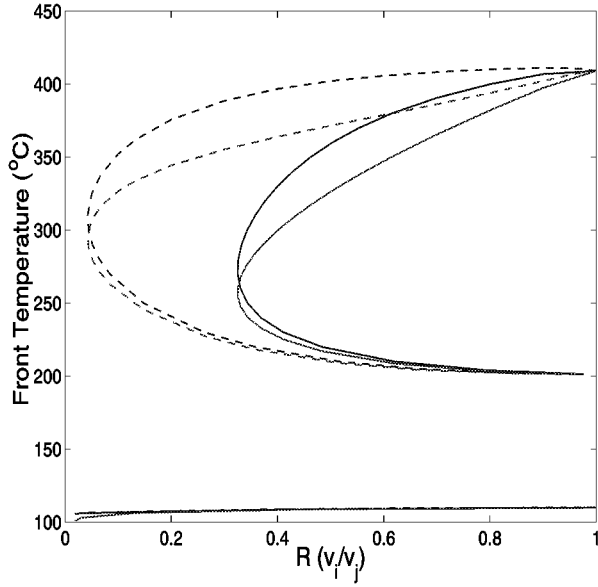


Figure 17: Nonadiabatic front temperatures for layers i and j versus R . Solid lines denote case j , dashed lines denote case i . $H_i=H_j=0.5\text{m}$, $\sigma=0.1$.

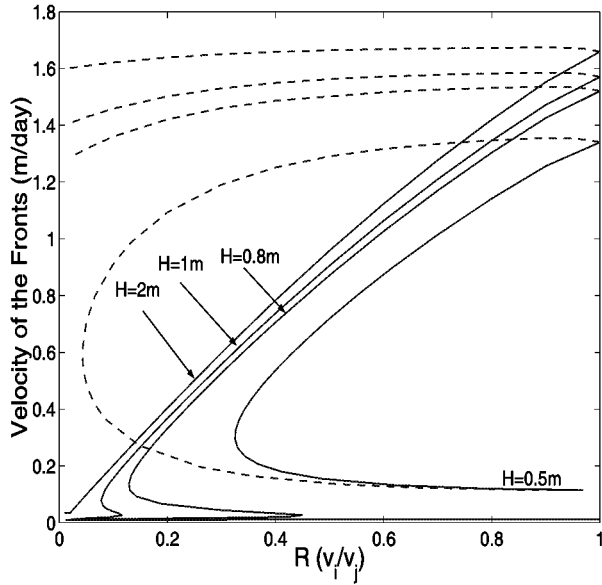


Figure 18: Nonadiabatic front velocity for layers i and j versus R for varying H . Solid lines denote case j , dashed lines denote case i . $\sigma=0.1$.

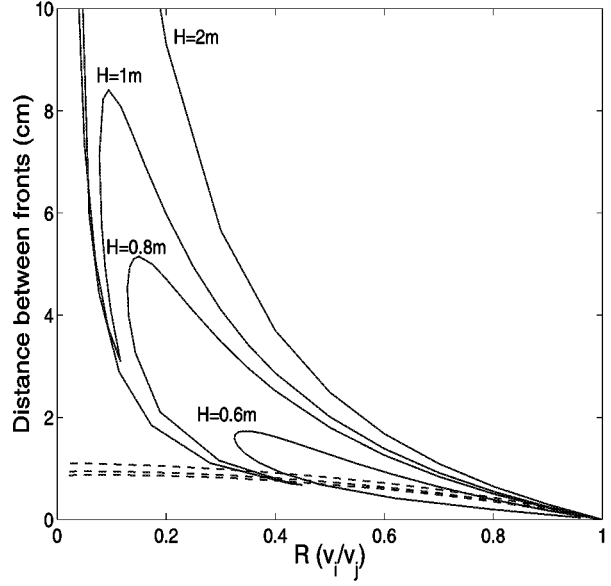


Figure 19: Distance between the fronts in layers i and j versus R for varying H and the non-adiabatic case. Solid lines denote case j , dashed lines denote case i . $\sigma=0.1$.

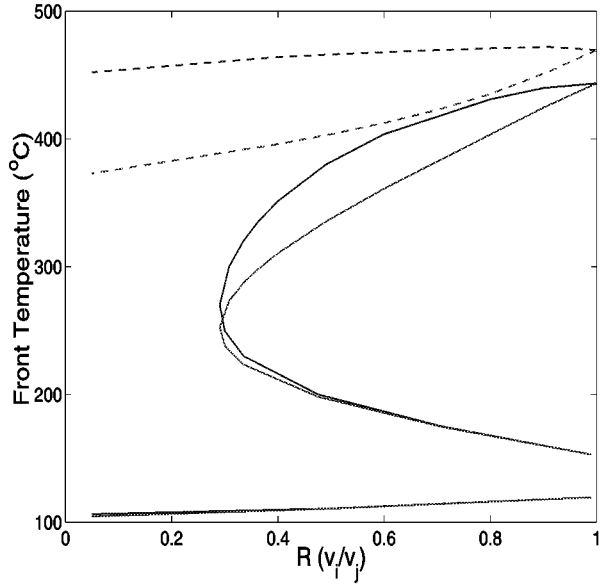


Figure 20: Front temperature versus R for the non-adiabatic symmetric, three-layer case. Solid line denotes thickness of the shielding layers equal to 0.5 m, dashed lines denote thickness equal to 2 m. $\sigma_i=0.1$

5 CONCLUDING REMARKS

In this report we extended the approach of [7] to heterogeneous systems, by considering the simpler case of in-situ combustion in layered porous media. Two simple geometries were considered, a two-layer model and a symmetric three-layer model. Analytical models were developed to delineate the combined effects of fluid flow, reaction and heat transfer on the dynamics of combustion fronts in the layers, using as parameters the thermal coupling between the layers, the heat transfer to the surroundings and the permeability contrast.

We find that in layered systems, the thermal coupling between layers leads to coherent traveling fronts, propagating at the same velocity. This coupling retards greatly fronts in the more permeable layer and accelerates only slightly those in the less permeable one, until a common front velocity is attained. In essence, the problem becomes slave to the injection velocity in the lower permeability layer. As in the single-layer case, there exists a unique solution, under adiabatic conditions, and multiple steady-state solutions, under non-adiabatic conditions. The latter lead to ignition and extinction conditions. Importantly, for a sufficiently large permeability contrast, relatively small layer thickness and under non-adiabatic conditions, steady-state propagation in the two layers cannot be sustained, and the process becomes extinct, even though, under the same conditions, sustained propagation would have been predicted for the equivalent single-layer problem with the average injection velocity. In a sense, the problem becomes controlled by the extremes of the permeability distribution. Such behavior can be detrimental to the success of in-situ combustion in highly heterogeneous layered media. In addition, it raises serious questions on the ability of conventional reservoir simulators to capture it. Conventional models average flow and kinetic behavior over substantially large distances, where effects, such as the above, which are dominated by the extremes of the permeability field, cannot be adequately represented. Precise conditions for the delineation of the above behavior need to be further developed. We anticipate that similar conclusions will hold in the case of heterogeneous media. Work in this direction is currently in progress.

References

- [1] Williams, F.A. *Combustion Theory*, Benjamin and Cummings Publishing Company Inc. (1985).
- [2] Britten, J.A. and Krantz, W.B., *Combust. Flame*, 60:125 (1985).
- [3] Britten, J.A. and Krantz, W.B., *Combust. Flame*, 65:151 (1986).
- [4] Schult, D.A., Matkowsky, B.J., Volpert, V.A., and Fernandez-Pello, A.C., *Combust. Flame*, 104:1 (1996).
- [5] Schult, D.A., Bayliss, A. and Matkowsky, B.J., *SIAM J. Appl. Math.*, 58:806 (1998).
- [6] Chuan, L. and Yortsos, Y.C. *A Pore-Network Model of In Situ Combustion in Porous Media*, paper SPE 69705 presented at the Society of Petroleum Engineers International Thermal Operations and Heavy Oil Symposium, Santa Margarita, Venezuela, March 15-17 (2001).
- [7] Akkutlu, I.Y. and Yortsos, Y.C. *Combust. Flame*, submitted (2001).
- [8] Willhite, G.P. *Waterflooding*, SPE Textbook Series Vol. 3 (1986)
- [9] Akkutlu, I.Y. *Dynamics of Combustion Fronts in Porous Media*, PhD Dissertation, U. of Southern California (2002, expected).

